

Optimization of Standard PMDC Motors used in Automotive Applications for Higher Power Density

Yannis L. Karnavas, Ioannis D. Chasiotis, Emmanouil D. Peponakis

Electrical Machines Laboratory, Department of Electrical & Computer Engineering
Democritus University of Thrace, Room 0.21, Building B, University Campus, Kimmeria,
Xanthi, 671 00, GR, Hellas

karnavas@ee.duth.gr, ichasiot@ee.duth.gr, emmapepo@ee.duth.gr

Abstract— Aim of this work is the development of a competitive alternate design topology (in terms of power density) of a small permanent magnet dc (PMDC) motor found in automotive applications. Initially, a real industrial motor is measured, designed and simulated, while its measurements and the relevant manufacturer data are considered as a benchmark. In turn, through custom developed software, a redesigned configuration is proposed regarding the structural (stator, rotor, magnets) geometry and magnet material. The resulting geometry was obtained through a constrained optimization algorithm having as goal the minimization of the overall volume and it was further verified by commercial finite element method (FEM) analysis software. Also, the new model is compared with the benchmark motor. Last but not least, FEM analysis was used for thermal behavior evaluation. The overall results reveal that the energy density and the performance of the proposed topology were substantially increased, while the cost was remained low.

Keywords—permanent magnet dc motors; electrical machine design; finite element method; automotive applications

I. INTRODUCTION

Despite the current trends where brushless direct current (BLDC) motors are now utilized in many application areas, permanent magnet dc commutator (PMDC) motors (which are common, basic types of dc motors), were traditionally and still being widely used in low cost automotive applications [1], [2]. They can be used for simple movement or precise speed and position control which is much cheaper than in case of BLDC counterparts. Sparks and interference from the brushes they wear may sometimes be an issue in some applications, but they are simple and cheap to drive, so they are many and quite common applications for them especially in automotive industry. Small rotating electric motors are an important part of a vehicle's electrical system and are used in several feature accessories. In a typical medium range vehicle there are usually 20-50 of them, while in a well equipped luxury vehicle there are over 100 such motors installed [3]. The list is impressive and can't be extensively reported here. Typical examples are: starter motor, radiator motor fan, air conditioning compressor drive, idle speed control, engine throttle control, electrically variable transmission, engine coolant pump motor, electrical valves, electro-hydraulic power steering, ABS systems, brake-by-wire actuators, active suspension actuator, windshield wipers, window lifts, seat

adjusters, seat vibrators, sunroof actuators, sliding door closers, headlamp adjusters, mirror adjusters, steering column adjuster, HVAC blower, cruise control, headlight wiper motors, power antenna, trunk closer, and auto-leveling systems. Also, it is obvious that the motors used in each case have very different requirements in terms of power, speed, torque, volume, form and size [4].

Problems associated with the optimization, analysis and performance of brushed PMDC motors have gained the focus of researchers over the last decades. The winding configurations combinations, the number of poles and the number of slots selection, the application of soft and hard magnetic materials, the collector and brushes transients and the efficiency maximization, have been studied and underline the problem significance [5]-[9].

Given this context, and the constant need for improving the electrical machines in general, the present work focuses on the design and analysis of a brushed PMDC motor as the mostly used motor type in small accessories for vehicles taking as a case study the windshield wiper motor. Once such an industrial motor is thoroughly tested and measured, an accurate 3D model of the original design is developed and analyzed in commercial FEM analysis software. At the same time, using custom software developed previously, the motor's specifications and other relevant data are taken into account for achieving an initial enhanced model which exhibits higher power density characteristics via an analytical dimensioning process. A key change in this stage, is the replacement of original ceramic magnets with neodymium ones. Also, for fair comparison reasons, the winding configuration (lap winding) is kept the same, although better performance of concentrated windings has been reported in literature [10]. Continuing, a further optimization stage is carried out by employing the FEM software capabilities to solve non-linear constrained optimization problems. Finally, the validation of the proposed optimized solution model is presented and discussed and a comparison is made with the original motor characteristics.

A brief theory reference along with the relevant problem formulation is presented in Section II, while the overall design procedure is discussed in Section III. Section IV reports and comments the derived results and finally Section V concludes the work. For clarity, a nomenclature is given in the Appendix.

II. BRIEF PMDC MOTOR THEORY & PROBLEM STATEMENT

A. Torque, Volume and Power Density Considerations

Fig. 1(a) shows a typical structure of a PMDC motor where it is seen that -apart from the commutator mechanism- there are essentially 4 parts: the rotor (formed by thin steel laminations), the copper windings, the magnets and the stator (or housing). Keeping in mind that the goal is to increase the power density of the motor, an increase to its output torque and/or a reduction to its volume are needed. Fig. 1(b) depicts a detailed cross-section where the key variables are shown. The PMDC motor's torque equation derivation along with key considerations follows (the reader can find details in [11]).

We recall that the specific magnetic loading (\bar{B}) is the average of the magnitude of the radial flux density over the entire cylindrical surface of the rotor. Also, the specific electric loading (\bar{A}) is the axial current per meter of circumference on the rotor. To obtain the total tangential force, we first consider an area of the rotor surface of width w and length L . The axial current flowing in the width w is given by $I = w\bar{A}$, and on average all of this current is exposed to radial flux density \bar{B} so the tangential force is given by Lorentz law as by $\bar{B} \times w\bar{A} \times L$ (it is assumed that current is perpendicular to the field). The area of the surface is wL so the force per unit area is $\bar{B} \times \bar{A}$. It is seen that the product of the two specific loadings expresses the average tangential stress over the rotor surface. To obtain the total tangential force a multiplication by the area of the curved surface of the rotor is needed, and to obtain the total torque, the total force should be then multiplied by the radius of the rotor. Hence, for a rotor of diameter D_r and length L , the total torque is given by

$$T = (\bar{B}\bar{A}) \times (\pi D_r L) \times \left(\frac{D_r}{2}\right) = \frac{\pi}{2} (\bar{B}\bar{A}) D_r^2 L \quad (1)$$

The term $D_r^2 L$ is proportional to the rotor volume, it is seen that for given values of the specific magnetic and electric loadings, the torque from any motor is proportional to the rotor volume. There is a liberty to choose a long thin rotor or a short fat one, but once the rotor volume and specific loadings are specified, the torque has been effectively determined. It is worth stressing that the above approach has not focused on any particular type of motor, but approached the question of torque production from a completely general viewpoint. In essence, the conclusions reflect the fact that all motors are made from iron and copper -and maybe hard magnetic material-, and differ only in the way these materials are disposed in space and interfere. Thus, different geometrical configurations and the use of certain material may affect dramatically the power density of a motor.

B. Problem Statement and Quantities under Concern

With respect to the previous paragraph, the problem statement and solution formulation can be given now. **Statement:** "Considering a given p -pole PMDC motor with a geometry as depicted in Fig.1(b), determine primarily the combination of D_r and L minimum values as well as the rest of parameters, so as to achieve the maximum power density while at the same time try to reduce the weight and improve the motor operational characteristics".

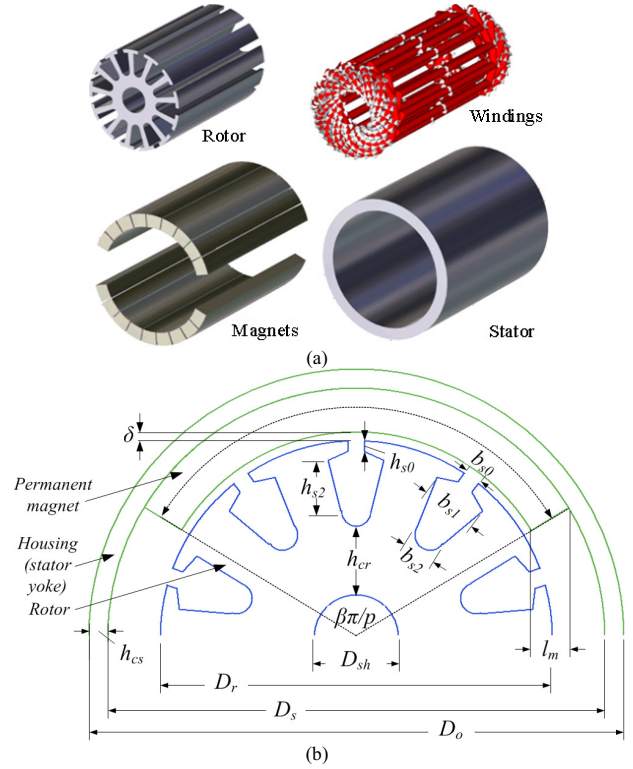


Fig. 1. Typical geometry of a PMDC motor, a) structural parts (commutator not shown), b) geometrical cross-section.

Solution Formulation: The area per pole is given by, $A_p = D_r L / p$. If Φ is the magnetic flux per pole, then

$$B = p\Phi / \pi D_r L \quad (2)$$

An increase of B increases the iron losses significantly but reduces the size and cost of the machine. Typical values for a PMDC motor lie between 0.3-0.7T and the upper limit is set by the phenomenon of saturation of magnetic material in stator teeth. Also, the specific electric loading can be obtained by,

$$A = I_z Z / \pi D_r \quad (3)$$

where $I_z = I_a / N$ is the current flowing in each conductor, I_a is the armature current, N is the number of conductors parallel paths and Z is the total number of conductors. An increase in A has the effect of reducing the cost and the size of the motor, while at the same time increases the copper losses, reduces the overload capacity and leads to an increase in motor's temperature. The power developed in the armature is given by:

$$P = E_a I_a = \frac{\Phi Z p n}{60 N} I_a \quad (4)$$

where E_a is the back-electromagnetic force and n is the motor's speed in rpm. Substituting (2) and (3) in (4) leads to

$$P = \pi^2 B A D_r^2 L \quad (5)$$

Eq. (5) is a relationship of D_r and L . Thus, another expression relating these two parameters is needed. This expression is the ratio of armature core length to pole pitch. In the most industrial PMDC motor this ratio lies between 0.55

and 1.1. The pole pitch τ refers to the circumferential distance corresponding to one pole at diameter D_r and can be calculated by:

$$\tau = \pi D_r / p \quad (6)$$

From this point on, the determination of the rest of the parameters can be conducted, i.e. the number of armature slots, their geometry and the selection of winding configuration. The number of armature slots Q_r depends on the number of poles. For example, in a 2-pole machine the slot pitch is 0.01 to 0.04 meters and therefore the number of slots varies from $(\pi D_r / 0.04)$ to $(\pi D_r / 0.01)$. Furthermore, the lap windings are a common choice through wave winding especially for small PMDC machines. Semi-closed round slots have been selected, as they are commonly used in commercial motors. Also, for the parameter b_{s0} is usually equal to 2mm. Finally, the geometry of the armature slots can be completed by using Eqs. (7)-(11):

$$h_{cr} = \Phi / 2B_{cr}L \quad (7)$$

$$h_{s2} = (D_r - D_{sh}) / 2 - h_{cr} - h_{s1} - h_{s0} \quad (8)$$

$$b_{tr} = p\Phi / Q_r B_{tr}L \quad (9)$$

$$b_{s1} = (\pi [D_r + 2(h_{s0} + h_{s1})] / Q_r) - b_{tr} \quad (10)$$

$$b_{s2} = (\pi (D_r - 2h_{cr}) / Q_r) - b_{tr} \quad (11)$$

In order to proceed with the stator part, the airgap length should be first calculated. It is well known that this parameter has significant effect on PMDC motor performance. Although there is technically no restriction on the minimum achievable airgap, an airgap length in the 1mm order of magnitude is usually chosen in this type of motors for economical reasons. The type and the shape of the magnets are also of great importance and depend on the cost factor, the availability, the mechanical properties and the desirable electromagnetic performance. The appropriate value of magnets length (l_m) and the pole-arc-to-pole-pitch ratio ($\beta\pi/p$) can be determined through parametric analysis or optimization procedure and FEM simulations in order to achieve the specific requirements. However, the final value of these parameters affects the total flux in the airgap. The dimension of the stator yoke ($h_{cs} = (D_o - D_s) / 2$) is determined by the value of the flux carried by the yoke. It is considered here that the yoke carries half of the total flux. The flux density of yoke for a permanent magnet motor should not exceed 0.8 Wb/m^2 . Finally, other geometrical parameters and characteristics such as the diameter and length of commutator, the width and thickness of the brushes and the commutator diameter and length can easily defined, as described in [12]-[14].

C. PMDC Motor under Study

Table I summarizes a few examples of vehicle accessories PMDC motor applications and the typical characteristics of each case. Among them, one can notice the wiper motors, which accelerate the wiper blades back and forth across the windshield. In order to make that happen, a great force is required and therefore a worm gear (usually with a 1:50 ratio) is used on the motor's shaft. The wiper motors provide a comparatively simple and reliable DC drive solution, as they

TABLE I. TYPICAL CHARACTERISTICS OF PMDC MOTORS APPLIED ON SOME VEHICLE ACCESSORIES

Application →	No. of Poles	No. of Slots	No. of Brushes	Speed (rpm)	Power (W)	Voltage (V)
Radiator Fan Motor	4	20	4	2565	150	12
Electro-hydraulic ABS Motor	2	12	2	1000	500	12
Electro-hydraulic Power Wiper Motor	4	21	4	2000	500-1500	12
Heater-Blower Fan Motor	2	10	2	1820	120	12
Starter Motor	6	29	2	1800	1200	12

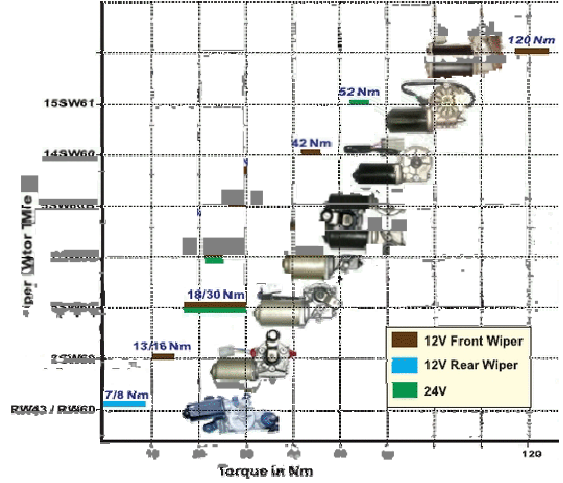


Fig. 2. Vehicle wiper motor power range chart according to manufacturers.

are powered by a 12V or 24V battery), combined with high starting torque. The starting torque can reach or exceed 175% of the rated torque and feature also a linear speed-torque curve. Typical manufacturer wiper motor torque range is depicted in Fig. 2. The most important characteristic of these motors is their small overall size, which provides substantial saving in both volume and weight. Their efficiency is relatively low and rarely exceeds 60% [15], [16].

Cylindrical slotted dc armatures are usually chosen, which are generally associated with stator poles made of low cost ceramic ferrite magnets, having a magnetic flux density near to 0.4T. In this case the magnets are longer than the armature core in order to provide axial flux concentration effect and increase the flux density in the armature.

The wiper motor studied here is a commercial PMDC motor, which will be considered as benchmark motor from now on. It is a 12V/32W, two-pole ceramic motor with rated speed and torque equal to 3,400rpm and 101mNm correspondingly. It “wears” 2 brushes, the commutator consists of 12 segments and there are 12 slots equipped with 30 conductors per slot. Fig. 3 depicts the overall assembly of the actual motor used as benchmark motor. Also, the motor design and performance characteristics are presented in Table II.

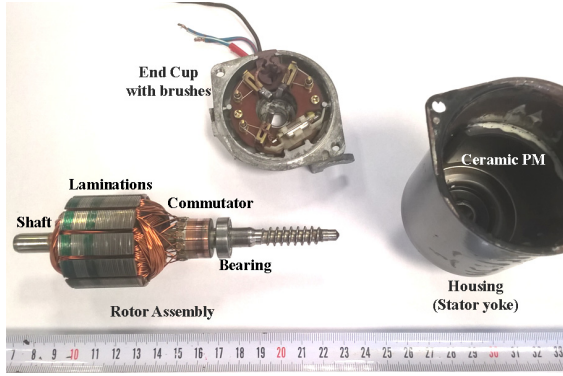


Fig. 3. Actual PMDC motor used and parts description.

III. DESIGN PROCEDURE

For the purpose of this work, a custom motor sizing program proposed recently in [17] was employed, using the starting equations given here and also the rest classical PMDC motor theory equations required. The program's knowledge base architecture is shown in Fig. 4. The main program inputs are a) the electrical/mechanical motor specifications e.g. input voltage, output power, gear ratio etc, b) the candidate materials properties e.g. mass densities, permeabilities etc, c) starting main sizing quantities e.g. number of poles and no. of slots, d) starting main geometrical dimensions and/or constraints e.g. inner and outer diameter of the motor), e) manufacturer datasheet information, f) thermal requirements e.g. maximum current density in coils, g) magnetic requirements e.g. flux densities in stator/rotor and the airgap).

Non-linear materials are also taken into account in the magnetostatic calculations. The resulting model is then validated by FEM. Actually, the motor was designed according to its geometrical dimensions and analytical calculations with the FEM software through 2D and 3D analysis were conducted, where in turn it was simulated in dynamic and steady state operation in order to compare the results obtained with those found by the analytical method. Further optimization of this model actually poses an optimization problem with several variables and constraints. Thus, the latter is solved by genetic algorithms method which is already embedded in the software. The main purpose of this optimization procedure is the reduction of the total volume of the redesigned motor, by minimizing the quantity $D_r^2 L$, while the main problem constraints and the motor specifications and performance requirements are also met as minimum. Moreover, the use of sintered NdFeB which have high energy content, instead of the ceramic ones, gave the opportunity to investigate the feasibility of the construction of higher power density topologies without performance degradation.

For the rest of the motor parts, silicon steel has been used for armature core and housing for both benchmark and redesigned motor, copper for armature windings and metallic graphite mixed with copper dust for the brushes in order to provide low voltage drop (approx. 1V per bush). The shaft diameter also remained the same, as well as the number of brushes and their dimensions, the number of commutator

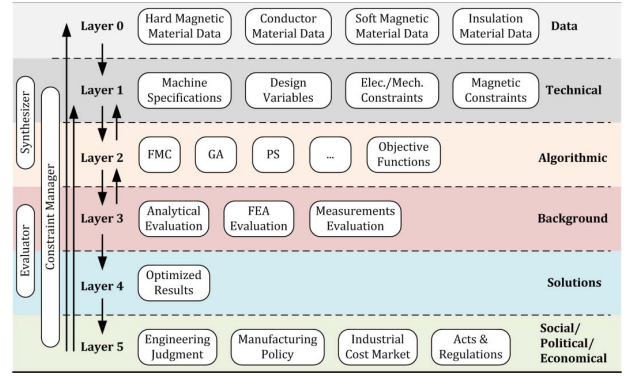


Fig. 4. Architecture of the electrical machines dimensioning knowledge based system developed previously and used here [17].

segments and its diameter and length. This choice is justified by the fact that the main purpose of this work is to design a PMDC motor with higher energy density, due only to the reduction of its size and the use of high energized magnets. In other words, a potential improvement of the motor performance due to a more appropriate design of the commutator is out of the current scope. Also, the commutator diameter, which usually is 0.5-0.9 of the armature's diameter, seems to fit the final proposed topology, as it will be shown in the next Section. Based on the above, it should be mentioned that the weight and the cost of the bearing, brushes and commutator have been excluded from the calculation of the total net weight of the motor and its total bulk cost.

IV. PROPOSED TOPOLOGY AND RELEVANT RESULTS

In this section the redesigned motor (and its validation), which derived through the already mentioned optimization procedure, is presented and compared to the benchmark motor. At first, the design variables and the structural characteristics, such as the total weight and bulk cost, of each case are given. Next a performance analysis of the two motors is shown and finally a thermal evaluation is also done in order to evaluate the good thermal behavior of the proposed motor.

A. Structural Optimization Results

The geometrical characteristics of the proposed and benchmark motor are shown analytically in Table II. Fig. 5 also depicts 3D model representations of both motors in common scale. It can be easily observed that a significant reduction of the total volume (46.3%) was finally obtained in the structure using sintered NdFeB magnets of residual flux density of 1.23T. The overall motor diameter and its active length are reduced by almost 19% and 21% respectively. This feature leads to a very important reduction of the total net weight of the motor by 46.56% and evaluates the design methodology and the applied optimization procedure. The power to weight ratio of the redesigned motor is increased and becomes almost twice compared to the original motor (87.2%), while the cost remains quite low for such performance. Additionally, less copper is used in the armature windings, while the weight of the NdFeB permanent magnets that is required in the second case is equal to only 25% of the magnets weight of the benchmark motor.

TABLE II. DESIGN RESULTS & OVERALL COMPARISON

	Benchmark PMDC Motor	Redesigned PMDC Motor	Percentage variation
Voltage (V) / No. of poles	12 / 2	12 / 2	-
Power (W) / Speed (rpm)	36 / 3400	36 / 2580	- / (-24.12%)
Rated Torque (mNm)	101.86	133.33	(+31.68%)
No. of brushes/ No. of slots	2/12	2/10	-
Active length L (mm)	34.10	27.00	(-20.82%)
Outer stator dia. D_o (mm)	61.40	50.00	(-18.57%)
Inner stator dia. D_s (mm)	54.60	40.00	(-26.74%)
Outer rotor dia. D_r (mm)	45.00	34.00	(-24.44%)
Shaft dia. D_{sh} (mm)	9.80	9.80	(0.00%)
Magnet length l_m (mm)	5.00	2.00	(-60.00%)
Airgap length δ (mm)	1.00	1.00	(0.00%)
Magnet arc ($\beta\pi/p$)	0.83	0.60	(-27.71%)
Slot opening width b_{s0} (mm)	2.00	2.00	(0.00%)
Slot top width b_{s1} (mm)	6.45	4.78	(-25.89%)
Slot base width b_{s2} (mm)	3.60	2.67	(-25.83%)
Slot height at top h_{s0} (mm)	1.25	0.50	(-60.00%)
Slot height at end h_{s2} (mm)	5.80	5.29	(-8.79%)
Permanent magnet type	Ceramic	NdFeB35	
Total net weight W (gr)	654.92	349.99	(-46.56%)
Copper weight W_c (gr)	95.59	78.34	(-18.04%)
Arm. core Weight W_a (gr)	210.74	97.04	(-53.95%)
PM weight W_m (gr)	113.83	28.62	(-74.86%)
Stator weight W_{st} (gr)	234.76	146.00	(-37.80%)
Bulk cost C (\$)	1.88	3.05	(+62.20%)
Volume V (cm ³)	128.55	67.50	(-46.30%)
Power density P_d (W/gr)	0.055	0.103	(+87.20%)

B. Performance Evaluation Results

The performance curves of both motors over the torque range are plotted and shown in Fig. 6. The rated torque of the optimized motor is substantially increased when compared to the original one for a given horsepower (31.68%). The motor's rated operation point is closer to the operation points of maximum output power and maximum efficiency, a characteristic that is desirable. The input current of the redesigned motor is always lower over the torque range compared to the corresponding one of the benchmark motor. The same is also observed for the starting current. The efficiency is slightly increased (52.1% in contrast with 50.6% of the initial motor) despite the fact that it was not included in the objective function of the optimization procedure. The losses distribution analysis revealed that the losses in brushes are the quite same in both cases, as the same design parameters have been used. The iron losses in the armature and stator core are also the same, while the frictional losses and the copper losses are significant lower in the second case. This feature is very interesting, as it seems that the important weight and volume reductions for wiper motors with NdFeB magnets can be combined with good performance.

The above are also confirmed by the magnetic flux density distributions which are depicted in Fig. 7. The flux density in the airgap and the magnets of the proposed topology is slightly higher than the corresponding one of the benchmark motor. This can be explained by the high energy content of the NdFeB magnets and justifies the increment of rated torque according to the Eq. (1). Moreover, important difference is observed in the flux distribution on the stator yoke in the second motor, which is desirable and guarantees that no saturation phenomenon will be developed for the soft magnetic material of the stator. It must be mentioned that stator yoke height was included in the constraints of the

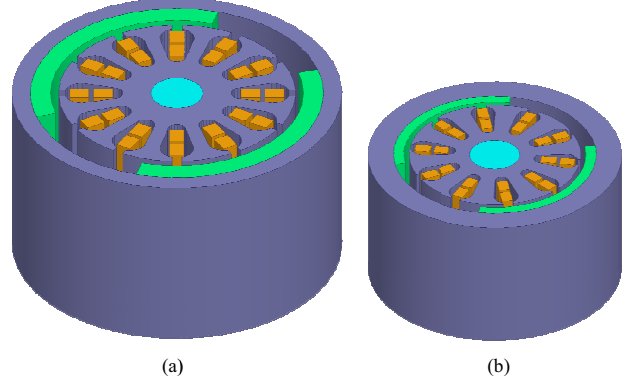


Fig. 5. 3D model representations of the PMDC under study, a) original motor, b) proposed redesigned motor (common scale).

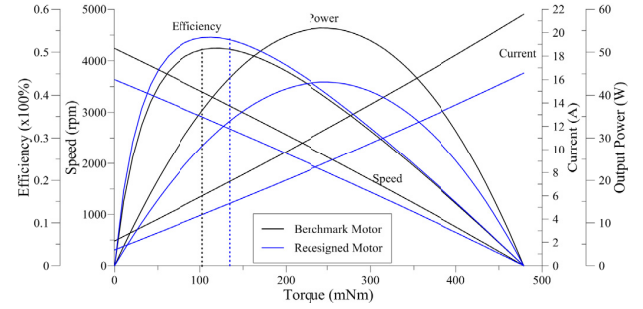


Fig. 6. Benchmark and redesigned PMDC motors performance charts (dotted lines denote nominal operating point).

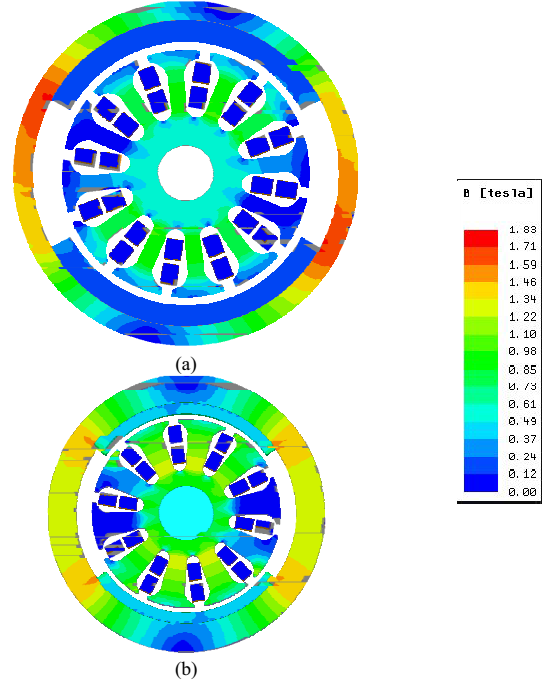


Fig. 7. Magnetic flux density distribution (radial cross section in common scale) in load condition, a) original motor, b) proposed redesigned and optimized motor.

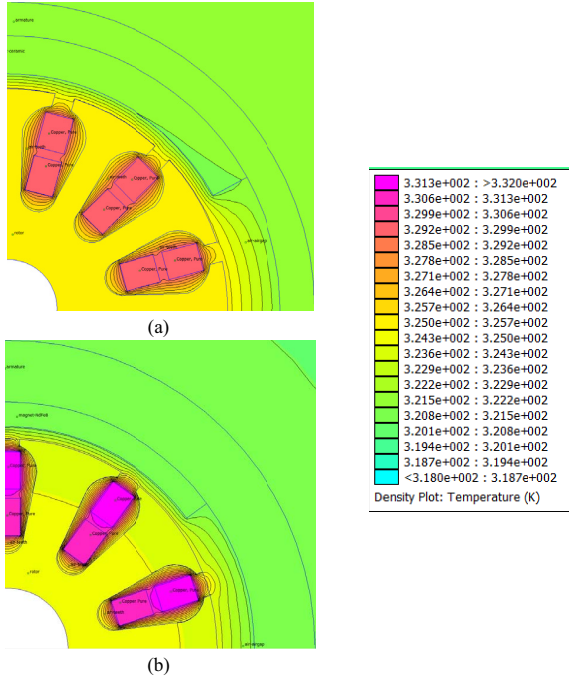


Fig. 8. Temperature distribution (radial cross-section not in common scale) in load condition, (a) original motor, (b) proposed redesigned and optimized motor.

TABLE III. PEAK TEMPERATURES DEVELOPED ON MOTOR PARTS

	Original Motor	Redesigned Motor	Variation
Rotor	321.2K (47.05°C)	322.4K (49.25°C)	+1.2°C
Windings	329.3K (56.15°C)	332.2K (59.05°C)	+2.9°C
Airgap	323.1K (49.95°C)	324.4K (51.25°C)	+1.3°C
Magnets	321.6K (48.45°C)	322.7K (49.55°C)	+1.1°C
Stator	324.2K (51.05°C)	325.3K (52.15°C)	+1.1°C

optimization procedure in order to ensure that both the mechanical and the magnetostatic requirements are met. The custom motor sizing program that was used or a related similar one can contribute to the development of even higher power density and more efficient PMDC motor for automotive applications, with new magnetic materials and motor structures with different number of poles and slots.

C. Thermal Evaluation Results

Generally the thermal behavior of a PMDC motor depends on the heat sources (such as copper, iron losses and brush losses) and the motor's geometry. A detailed thermal analysis is essential in order to find out if the heat distribution is able to provoke serious failures, such as the breakdown of the insulation surrounding the copper windings and the demagnetization of the magnets. The magnet temperature is an important item to be calculated especially when NdFeB magnets are to be used, as they are more sensitive to demagnetization at elevated temperatures than other rare earth magnets. Visualization instants of both motors operation under nominal load are shown in Fig. 8, while the peak temperatures observed on each part of the motors are given in Table III. The maximum temperature rise is about 332K for the proposed

topology. The results are judged absolutely satisfactorily and demonstrate that the reduction of the volume of the motor was not accompanied by any significant increase in temperature.

V. CONCLUSIONS

Brushed PMDC motors play a vital role in automotive applications. Industrial motors which are widely available in the market utilize superficially -for the sake of cost benefit- the classical design theory while using cheap materials, thus in some cases exhibit not so efficient power to volume/weight ratio. This study confronted with the structural and power density optimization of a small PMDC motor and proposed an alternative topology using 3D FEM analysis validation. Thermal investigations were conducted also. The redesigned motor results reveal that the energy density of the proposed topology was substantially increased by a factor of over 87% while keeping the overall cost within affordable limits for the manufacturer.

VI. APPENDIX: LIST OF SYMBOLS

\bar{A}	, specific electric loading,
A_p	, area per pole,
\bar{B}	, specific magnetic loading,
B_{cr}	, flux density in rotor yoke,
B_{cs}	, flux density in stator yoke,
B_{tr}	, flux density in rotor teeth
b_{s0}	, slot opening width
b_{s1}	, slot top width
b_{s2}	, slot base width
b_{tr}	, rotor tooth width
C	, bulk cost
D_o	, outer stator diameter
D_r	, rotor diameter
D_s	, inner stator diameter
D_{sh}	, shaft diameter
E_a	, back electromagnetic force
h_{s0}	, slot height at top
h_{s2}	, slot height at end
h_{cr}	, rotor yoke height
h_{cs}	, stator yoke height
I, I_a	, axial and armature current
L	, motor active length
l_m	, magnet length
N	, number of conductors parallel paths
p	, number of poles
P	, power developed in the armature
P_d	, power density
Q_r	, number of rotor slots
T	, torque
V	, volume
W	, total net weight
W_a	, armature copper weight
W_c	, armature core weight
W_m	, permanent magnet weight
W_y	, stator yoke weight
Z	, total number of conductors
$\beta\pi/p$, pole-arc to pole pitch ratio
δ	, airgap length
Φ	, magnetic flux per pole
τ	, pole pitch

References

- [1] J.M. Cheng, L. Sun, G. Buja, and L. Song, "Advanced Electrical Machines and Machine-Based Systems for Electric and Hybrid Vehicles", *Energies*, vol. 8, 2015, pp. 9541-9564.
- [2] Y.L. Karnavas, I.D. Chasiotis and S.K. Amoutzidis, "Design Considerations and Analysis of In-Wheel Permanent Magnet Synchronous Motors for Electric Vehicle Applications using FEM", in *Proc. of 17th Int. Symposium on Electromagnetic Fields in Mechatronics, Electrical and Electronic Engineering (ISEF)*, Valencia, Spain, Sep. 10-12, 2015, cd ref. no. GR082.
- [3] H. Thieme, "Influence of Automotive 42V Powernet on Small PM DC Motors", in *Proc. of IEEE Int. Conference: Electric Machines and Drives Conference (IEMDC)*, Cambridge, MA, USA, June 17-20, 2001, pp. 591-593.
- [4] C.P. Cho and R.H. Johnston, "Electric motors in vehicle applications", in *Proc. of the IEEE Int. Vehicle Electronics Conference (IEVC)*, 1999, vol. 1, pp.193-198.
- [5] D. Parente, M. Villani, "Noise Reduction in Permanent Magnet DC Motor for Rear Wiper", in *Proc. of IEEE Int. Electric Machines and Drives Conference (IEMDC)*, Cambridge, MA, USA, June 17-20, 2001, pp. 582-584.
- [6] J. Junak, G. Ombach, and D. Staton, "Permanent Magnet DC Motor Brush Transient Thermal Analysis", in *Proc. of the 18th Intl. Conference on Electrical Machines (ICEM)*, Vilamora, Portugal, Sep. 6-9, 2008, paper id. 1109.
- [7] G.C.R. Sincero, J. Ghannou, J. Cros, and P. Viarouge, "Collector model for simulation of brush machines", *Mathematics and Computers in Simulation*, vol. 81, 2010, pp. 340-353.
- [8] K. Hot, and P. Bodlovic, "Multi-Objective Optimization of Permanent Magnet Motor Using Taguchi Method", in *Computer Engineering in Applied Electromagnetism* (eds. S. Wiak, A. Krawczyk, M. Trlep), Springer, 2005, pp. 53-58.
- [9] M. Kasper, K. Hameyer, A. Kost, "Automated optimal design of a permanent magnet DC motor using global evolution strategy and FEM", *Int. Journal of Applied Electromagnetics and Mechanics*, vol. 6, 1995, pp. 367-376.
- [10] J. Cros and P. Viarouge, "Synthesis of high performance PM motors with concentrated windings", *IEEE Transactions in Energy Conversion*, vol. 17, no. 2, 2002, pp. 248-253.
- [11] A.E. Miller, E.F. Richards, A.W. Yeadon, W.H. Yeadon, "Direct Current Motors", book chapter in *Handbook of Small Electric Motors*, (A.W. Yeadon, W.H. Yeadon eds.), McGraw Hill, USA, 2001.
- [12] J. Cros, G.C.R. Sincero, P. Viarouge, "Design Method for Brush Permanent Magnet DC Motors", in *Proc. of Intl. Conf. on Electrical Machines and Drives Conference (IEMDC' 09)*, May 3-6, 2009, Miami, pp. 1625-1632.
- [13] S.S. Yegna Narayanan, K.R. Anandakumaran Nair, V. Narayanan, "Design Analysis of Permanent Magnet D.C. Motors with Differing Armature, Magnet and Yoke Lengths", *IEEE Trans. on Energy Conversion*, vol. 13, no. 1, March 1998, pp. 55-61.
- [14] C.C. Hwang, J.J. Chang, "Design and analysis of a high power density and high efficiency permanent magnet DC motor", *Journal of Magnetism and Magnetic Materials*, vol. 209, 2000, pp. 234-236.
- [15] F.N. Klein, M.E. Kenyon, "Permanent Magnet DC Motors Design Criteria and Operation Advantages", *IEEE Trans. on Industry Applications*, vol. 20, no. 6, Nov. 1984, pp. 1525-1531.
- [16] K. Hameyer, R.J.M. Belmans, "Permanent Magnet Excited Brushed DC Motors", *IEEE Trans. on Industrial Electronics*, vol. 3, no. 2, April 1996, pp. 247-255.
- [17] Y.L. Karnavas and I.D. Chasiotis, "A Simple Knowledge Base Software Architecture for Industrial Electrical Machine Design: Application to Electric Vehicle's In-Wheel Motor", in *Proc. of 36th Int. Conference on Information Systems Architecture and Technology (ISAT)*, Karpacz, Poland, Sep. 20-22, 2015, cd ref. no. 58.